JACS
JOURNAL OF THE AMERICAN CHEMICAL SOCIETY

Article

pubs.acs.org/JACS

Spontaneous Thermoreversible Formation of Cationic Vesicles in a Protic Ionic Liquid

Carlos R. López-Barrón,[‡] Dongcui Li, Leo DeRita, Madivala G. Basavaraj,[¶] and Norman J. Wagner*

Center for Neutron Science, Department of Chemical and Biomolecular Engineering, University of Delaware, Newark, Delaware 19716, United States

Supporting Information

ABSTRACT: The search for stable vesicular structures is a long-standing topic of research because of the usefulness of these structures and the scarcity of surfactant systems that spontaneously form vesicles in true thermodynamic equilibrium. We report the first experimental evidence of spontaneous formation of vesicles for a pure cationic double tail surfactant (didodecyldimethylammonium bromide, DDAB) in a protic ionic liquid (ethylammonium nitrate, EAN). Using small and ultra-small angle neutron scattering, rheology and bright field microscopy, we identify the coexistence of two vesicle containing phases in compositions ranging from 2 to 68 wt %. A low density highly viscous solution containing giant vesicles ($D \sim 30\ \mu$m) and a sponge (L_3) phase coexists with a dilute high density phase containing large vesicles ($D \sim 2.5\ \mu$m). Vesicles form spontaneously via different thermodynamic routes, with the same size distribution, which strongly supports that they exist in a true thermodynamic equilibrium. The formation of equilibrium vesicles and the L_3 phase is facilitated by ion exchange between the cationic surfactant and the ionic liquid, as well as the strength of the solvophobic effect in the protic ionic liquid.

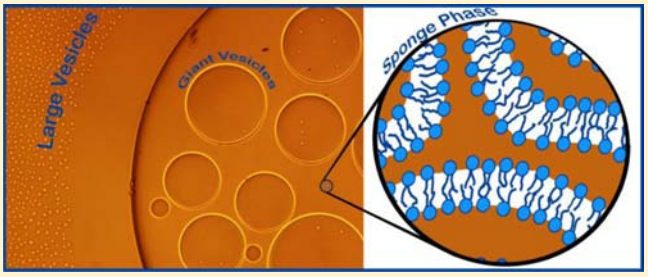

INTRODUCTION

Most vesicular structures are formed by the input of external energy on a planar lamellar phase (e.g., by sonication[1] or mechanical filtration[2]). The stability of these structures is kinetically limited because the starting components (typically phospholipids or dialkyldimethylammonium halides) are highly insoluble, and therefore, the collapsed planar lamellar is the equilibrium state of aggregation.[3,4] The metastability of these vesicles limits their usage as drug carriers, as microreactors or as models for biological membranes.[5] Their size and distribution depend on the specifics of their processing and can be difficult to reproduce. Spontaneously formed equilibrium vesicles would be greatly preferred for these applications. However, only few reports of spontaneous vesicle formation on systems with a single surfactant can be found in the extensive literature on phospholipids and liposomes. Grillo and co-workers[6] reported the existence of micelles and multilamellar vesicles in didodecyldimethylammonium bromide (DDAB)/water solutions at very low concentrations. They reported a critical micellar concentration, cmc = 4.63×10^{-2} mmol/L (0.002 wt %) and a critical vesicle concentration, cvc = 7.34×10^{-1} mmol/L (0.03 wt %). DDAB in water can also be induced to form multilamellar vesicles by ultrasonication.[1] However, to date, there are no reports of spontaneous unilamellar vesicle formation in the absence of a cosurfactant. Given the interest in using ionic liquids as "green solvents", developing a spontaneous vesicle forming system in an ionic liquid is highly desirable.

One route to achieve spontaneous formation of stable vesicles is by mixing cationic and anionic surfactants (catanionic surfactants).[5,7−12] For instance, spontaneous vesicle formation was observed in the DDAB-containing catanionic mixtures: sodium dodecylbenzene sulfonate (SDBS)/DDAB/H2O[11,12] (in the DDAB-rich dilute region of the phase diagram), and sodium dodecyl sulfate (SDS)/DDAB/H2O[9] (in both DDAB-rich and SDS-rich dilute regions). Evans and co-workers showed that vesicles can also form spontaneously in aqueous solutions when the bromide counterion in DDAB is substituted by a more hydrophilic ion (e.g., OH^-), which results in larger surfactant headgroup area and increased spontaneous curvature.[13,14] A similar effect was reported by Murthy et al., in mixtures of the ionic surfactant Aerosol OT and cholinergic salts.[15]

Ionic liquids are poorly coordinated salts with melting points (mp) below 100 °C. Because of the protic nature and general solvent properties (such as polarity), protic ionic liquids (PILs) have greater similarity to water than aprotic ionic liquids (AIL). For instance, ethylammonium nitrate (EAN, a PIL with mp = 14 °C) shares many properties with water including formation of a three-dimensional hydrogen bond network.[16,17] Thus, EAN is suitable for use as self-assembly media where the self-assembly is driven by solvophobic interactions. Recent studies have reported self-assembly in EAN, including micellization[18,19]

Received: September 13, 2012
Published: October 3, 2012

and liquid crystal formation.[20−22] The only previous report of vesicle formation in ILs (where the IL acts as solvent) is of dialkyldimethylammonium amphiphiles in (ether-containing) immidazolium-based AILs by Nakashima and Kimizuka.[23] Formation of stable vesicles has been observed in ternary solutions, where an IL acts as cosurfactant.[24−26] Recently, Bai and Lodge[27] described spontaneous formation of poly(butadiene-b-ethylene oxide) block copolymer polymersomes (polymer vesicles) in an hydrophobic aprotic immidazolium-based IL. Vesicle formation in protic ionic liquids has not been reported to date. In this article, we report that solutions of DDAB in EAN spontaneously form thermodynamically stable vesicles.

RESULTS AND DISCUSSION

Phase Behavior of DDAB/EAN Solutions. The phase diagram of purified DDAB in dry EAN, mapped by visual inspection of samples immersed in an oil bath, is shown in Figure 1. Single transparent phases are observed in concentration ranges [DDAB] ≤ 1.9 wt % and 68 wt % < [DDAB] < 80 wt %. These phases, identified as dissolved monomers and a sponge (L_3) phase, respectively, coexist in the range 1.9 wt % < [DDAB] < 68 wt % (see inset in Figure 1). The upper phase (UP) is more concentrated and hence has a higher viscosity than the lower phase (LP) (the rheological responses of both phases are discussed in the Supporting Information). It is noteworthy that the phase boundaries are vertical, that is, samples with compositions near 1.9 or 68 wt % do not mix or phase separate by heating or cooling within the temperature range studied. This indicates that the critical point (if there is any) is at a temperature higher than 120 °C. This temperature was not surpassed to avoid decomposition of EAN. The vesicle/L_3 phase coexistence region shown in Figure 1 is analogous to that observed by Segota and co-workers in the ternary SDBS/DDAB/H_2O system.[11,12] They observed vesicle formation in the dilute DDAB-rich region and coexistence of vesicles and a solid phase at molar ratios (n_{SDBS}/n_{DDAB}) ranging from 0.05 to 0.5. The formation of the solid phase may be due to the low solubility of DDAB in water. In contrast, the enhanced DDAB solubility in EAN leads to the swollen L_3 phase in concentrated DDAB/EAN solutions.

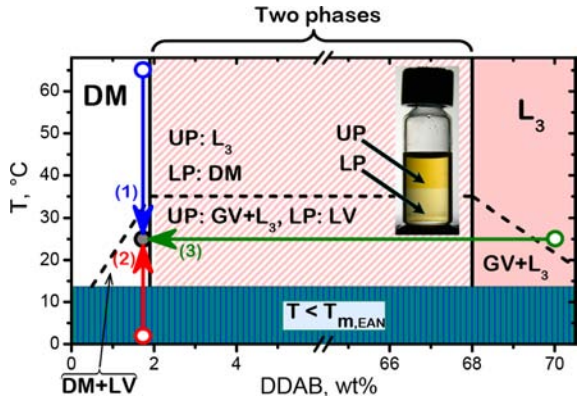

Figure 1. Temperature−composition phase diagram of DDAB/EAN. LP = lower phase, UP = upper phase, DM = dissolved monomers, LV = large vesicles, GV = giant vesicles, and L_3 = sponge phase. Inset picture: 30% DDAB/EAN solution showing the two separated macrophases. The dashed line marks the formation/destruction of both LV and GV. Long arrows connecting circles depict three different routed leading to LV formation (see Supporting Information).

At compositions beyond 80 wt %, a birefringent lamellar (L_α) phase and an opaque solid phase were observed. The characterization of the L_3 (sponge) and L_α phases is reported in a previous publication.[28] The phase behavior of DDAB in EAN is different to that observed for DDAB in water.[4,29,30] First, a lamellar phase (L_α) in DDAB/EAN solutions is observed only at very high compositions ([DDAB] ≥ 80 wt %), whereas in water, lamellar spherulites are found at concentrations as low as 0.5 wt % and a swollen L_α phase at 3 wt %. Second, a stable sponge (L_3) phase forms in DDAB/EAN solutions over a wide range of compositions (1.9 wt % < [DDAB] < 80 wt %), whereas in water, the L_3 phase exist only as a metastable state in very dilute aqueous solutions ([DDAB < 3 wt %).[3]

The two phases in samples within the coexistence region were extracted using a separatory funnel and characterized separately. The separated fractions are identified by their weight % and the phase position (e.g., DE30LP and DE30UP are 30 wt % DDAB/EAN lower and upper phases, respectively). The 1.8 wt % (DE2) and 68 wt % (DE68) solutions were also analyzed . Vesicles are observed at room temperature, using bright field microscopy (BFM), at concentrations [DDAB] < 68 wt %. DDAB vesicles are spontaneously formed in EAN by direct contact of the two components (see Supporting Information for a movie showing spontaneous formation of vesicles). In contrast, aqueous DDAB vesicles require the input of external energy to form.[1,3,4] The vesicles (in all the phases) disappear upon heating the solutions above 35 °C, and reform with a low polydispersity (see Table 1 and Figure 2) after lowering the temperature to T < 35 °C. The vesicle formation/dissolution is indicated by the dashed line in Figure 1 (see Supporting Information for movies showing the thermoreversible formation of LV and GV). Large vesicles (LV, $D \sim 2.8$ μm) form in both DE2 and DE30LP, whereas giant vesicles (GV, $D \sim 30$ μm) form in DE30UP and DE68, as indicated in the phase diagram (Figure 1). The vesicles in all phases are stable (>1 week) under quiescent conditions. Vesicles similar to those observed in the 30 wt % sample form across the entire range of compositions in the two phase region, as documented in the Supporting Information.

Table 1. Parameters from BFM Analysis and from SANS Modeling for the DE2 and DE30LP at 25 °C[a]

	BFM			SANS							
sample	D_c (μm)	PDI	$\Phi_s \times 10^3$	D_c (±0.02) (μm)	PDI (±0.02)	$\Phi_s \times 10^3$ (±0.01)	$\rho_c \times 10^6$ (±0.02) (Å^{-2})	$\rho_m \times 10^6$ (±0.02) (Å^{-2})	γ	ϕ_c	ϕ_m
DE2	3.09	0.22	0.95	2.62	0.24	1.1	3.46	3.54	1.09	0.034	0.013
DE30LP	2.87	0.21	1.2	2.49	0.22	1.4	3.42	3.53	1.12	0.043	0.015

[a]Note: Φ_s from BFM was computed using δ = 2.1 nm and Φ_s from SANS was obtained using the scale factor of the core-shell model fitting.

dx.doi.org/10.1021/ja308975e | J. Am. Chem. Soc. 2012, 134, 20728−20732

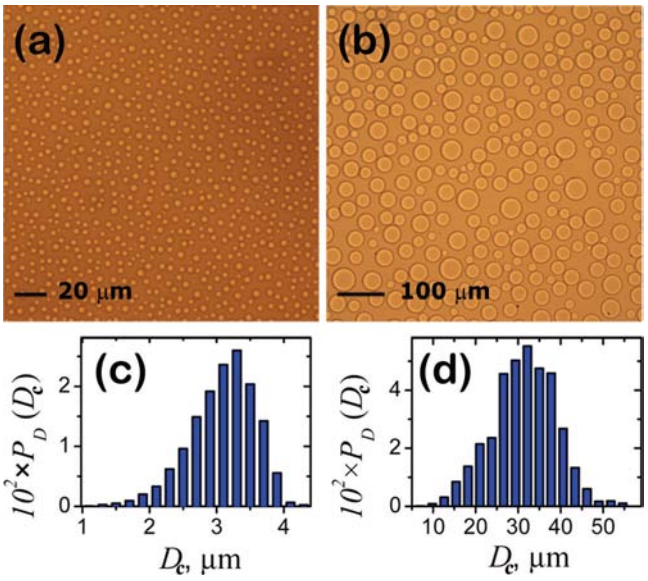

Figure 2. Micrographs recorded at 25 °C (upper row) and vesicle diameter distributions (lower row) for the lower phase (a and c) and the upper phase (b and d) of 30 wt % DDAB/EAN solution.

The core diameters, D_c, of more than 1500 vesicles in each sample were measured from the BFM micrographs using ImageJ. The diameter density distributions of DE30LP and DE30UP are shown in Figure 2c,d. The vesicle mean diameter, $\bar{D}_c$, and polydispersity (defined as PDI = $2\sigma/\bar{D}_c$, where σ^2 is the variance of the distribution) of LVs and GVs are given in Table 1 and Table S2, respectively. To verify that the vesicles are a true thermodynamic equilibrium state, rather than a kinetically trapped system (as is the case of many vesicular systems[31−34]), three different routes to the state of LV formation [25 °C, 1.8 wt %] are explored (see arrows connecting circles in Figure 1): (1) Cooling from 65 to 25 °C, (2) heating from 2 to 25 °C, and (3) diluting from a concentration of 70 wt % (corresponding to single L_3 phase) to 1.8 wt %. The three routes lead to similar vesicle size distributions, whereas no vesicles are observed at any of the three initial states (i.e., [65 °C, 1.8 wt %], [2 °C, 1.8 wt %], and [25 °C, 70 wt %]), as discussed in the Supporting Information.

Structural Analysis of the Large Vesicles. Figure 3 shows small and ultra-small angle neutron scattering (SANS and USANS) data for the DE30LP sample at 25 and 80 °C. At 25 °C, strong scattering is observed at low q values

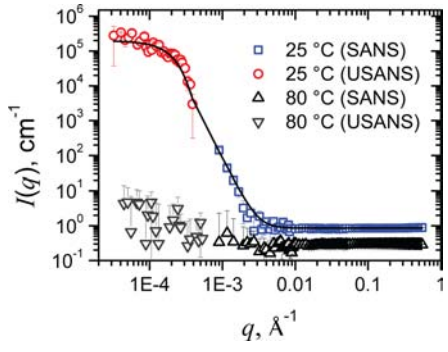

Figure 3. SANS and USANS data for the DE30LP sample at 25 and 80 °C. The solid line is a fit to the Core Shell model (eq 1) with a Schultz distribution.[35].

corresponding to vesicle shells (see Figure 2a). Negligible scattering is observed from the sample at 80 °C, indicating that, at this temperature, the DDAB molecules are in solution as monomers. The dissolution of vesicles upon heating was also observed by BFM (see Supporting Information for a movie showing the thermoreversible formation of LV and GV). Nearly identical scattering profiles are obtained from the DE2 sample. Unfortunately, due to the low scattering cross section for the USANS data at $q > 5 \times 10^{-4}$ Å^{-1}, these data are statistically unsuitable to be considered in the fitting. Therefore, there is a gap in q-range between SANS and USANS. However, no additional features are expected to be observed in the gap between 5×10^{-4} and 1×10^{-3} Å^{-1}. Scattering data from DE30LP and DE2 samples are analyzed using the form factor amplitude function based on core−shell structures with core radius $D_c/2$ and shell thickness δ[35]

$$F(q) = \frac{4\pi}{q^3}(\rho_s - \rho_c)[\gamma j(x + \delta) - j(x)] \quad (1)$$

where the function $j(x) = \sin x - x \cos x$ and $x = qD_c/2$. ρ_i is the scattering length density (SLD) of i (with c = core, s = shell, and m = medium). The scaled medium contrast, $\gamma = (\rho_m - \rho_s)/(\rho_c - \rho_s)$, determines the relative proportion of the scattering from the core and the shell. The polydispersity of the vesicles is accounted by averaging the form factor with a Schultz distribution.[35] Figure 3 shows the fit to the polydisperse core−shell model for the DE30LP sample. A single set of parameters (given in Table 1) was used to fit both SANS and USANS data. The core diameter obtained by the fitting is slightly smaller to that obtained by microscopy, while the polydispersity is comparable.

The volume fraction of the shell is calculated from microscopy with $\Phi_s = A_{A,s}$, where $A_{A,s}$ is the volume area fraction of the shell obtained optically, and compared to the value obtained from the fit to the core−shell model. These values, shown in Table 1, agree to within ∼15%, and are noticeable small compared to the total surfactant volume fraction, ∼ 0.02 (see Supporting Information).

It is not possible to fit the scattering data with the same SLD value for the core and the medium. Considering the SLD values for EAN and DDAB ($\rho_{EAN} = 3.59 \times 10^{-6}$ Å^{-2} and $\rho_{DDAB} = -2.77 \times 10^{-7}$ Å^{-2}), the reduced values of ρ_c and ρ_m (Table 1), coupled with the fact that only ∼0.1% of the surfactant is at the vesicle shells, indicates that most of the surfactant is dissolved or forming very small aggregates in both the core and the medium. The local volume fraction of the core, ϕ_c, and the medium, ϕ_m, are computed recognizing that the SLD is proportional to the mass density, and shown in Table 1. The observation that $\phi_c > \phi_m$ could be due to a higher local concentration near the vesicle shells induced by an adsorption/desorption equilibrium. Alternatively, it may be due to shape and size fluctuations, which are not taken into account in the core−shell model used here. Complementary experiments (e.g., dynamic light scattering) are required to characterize these fluctuations.[36] The lowering of the SLD of the medium could be explained by the presence of small aggregates. If we assume a critical aggregation concentration (for the vesicle formation) 10 times higher in EAN than in water (cmc and cvc in water are 4.63×10^{-5} mol/L and 7.34×10^{-4} mol/L, respectively[6]), as shown in ref 18 (for micelle formation), then the cvc in EAN can be expected to be around 7 mmol/L ($\phi \sim 3.4 \times 10^{-3}$). The volume fraction of DDAB in the medium is ∼4 times the value of the estimated cvc, which could be explained if much smaller

dx.doi.org/10.1021/ja308975e | J. Am. Chem. Soc. 2012, 134, 20728−20732

aggregates, such as micelles (not detected by BFM), coexist with the vesicles. Unfortunately, due to the high incoherent background of the system (~ 1 cm^{-1}), SANS measurements are not sensitive to the presence of micelles at such low concentration. Surface tension measurements would help to elucidate the formation and coexistence of micelles and vesicles, as shown previously in the analogous aqueous system by Grillo and co-workers.[6]

Structural Analysis of the Giant Vesicles and the Sponge (L_3) Phase. For the concentrated samples (DE30UP and DE68), the shell of the giant vesicles (Figure 2b) is not detected by SANS or by USANS, due to two reasons: (1) the vesicle size is beyond the instrument size resolution, and (2) given that δ = 2.1 nm (see Supporting Information), the surfactant in the shell represent just 0.01% of the total surfactant. Consequently, no scattering was detected at low q-values. However, a broad peak was observed at high q-values (shown in Figure 4). These samples are optically isotropic (i.e., dark under cross-polarizing microscopy), suggesting that the surfactant is forming a (sponge) L_3 phase.[28] This hypothesis was confirmed by fitting the SANS data with the Teubner–Strey (TS) model:[37] $I(q) = [a_2 + c_1q^2 + c_2q^4]^{-1}$. The composition-dependent coefficients a_2, c_1, and c_2 can be used to calculate the domain periodicity, d, and the correlation length, ξ, which is a measure of the short-range order among the domains (Table S2). The TS model fits well the scattering data of the DE30UP (Figure 4) and DE68 samples at 25 and 80 °C, and the computed values of d (Table S2) are comparable to the bilayer thickness (2.1 nm[28]). The average thickness of the EAN channels in the L_3 phase (see inset in Figure 4) and the volume fraction are calculated with $\delta_{EAN} = d - \delta$ and $\Phi_{L_3} = \delta/d$, respectively, and reported in Table S2.

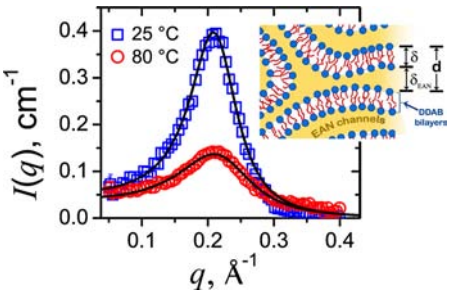

Figure 4. SANS data of the DE30UP sample at 25 and 80 °C. Solid lines are fits to the Teubner–Strey model.[37] The inset show a schematic of the L_3 DDAB bilayer structure in EAN.

The mass balance on the 30 wt % sample (given in the Supporting Information) indicate that this sample splits into two phases with concentrations corresponding to the phase boundaries (Figure 1). The swelling behavior of the L_3 phase at higher compositions ([DDAB] > 68 wt %) is reported elsewhere.[28] The phase split indicates that the system reaches a maximum swelling at [DDAB] ~68 wt %. That is, further dilution at this concentration does not increase the values of δ_{EAN} in the sponge phase. Rather, the excess EAN forms a second phase (the dilute LP phase), in equilibrium with the L_3 phase. Notice that the peak intensity at 80 °C (Figure 4) is lower than at 25 °C, indicating weaker correlation between DDAB bilayers at high temperatures, which may be also related to the formation/dissolution of the GVs.

Molecular Bases for Spontaneous Vesicle Formation. Even though the vesicles form spontaneously, their large size indicates that the bilayers are, on a molecular basis, effectively planar. That is to say, the product of the maximum dimension of the amphiphilic molecule, L, and the vesicle curvature, c, is $cL \ll 1$, which defines large unilamelar vesicles in contrast to small lamellar vesicles, for which $cL \sim 1$. For DDAB in water, Evans and co-workers suggested that the formation of vesicles (with diameters ~500 nm) upon replacing the counterion Br^- by OH^- in DDAB is a result of a reduction in the packing parameter, $p = v/a_0l_c$ (where v is the surfactant tail volume, l_c is the tail length, and a_0 is the area of the headgroup), which results in an increase in the spontaneous curvature.[13,14] The mechanism of aggregation of DDAB/EAN vesicles may be analogous to that of DDA–OH vesicles,[13,14] namely, the anion NO_3^- from EAN competes with the counterion Br^- (as suggested by Graves and Drummond for the CTAB/EAN system[38]). Note, however, that the DDAB vesicles in EAN are substantially larger than those observed in water. The degree of ion exchange (i.e., the Br^-/NO_3^- ratio) in the palisade layer of the bilayer can be different inside and outside of the vesicle because the compositions of the medium is different inside and outside, as demonstrated by SANS. This fact and the difference in screening strength between Br^- and NO_3^- allows a difference in spontaneous curvature between the inside and outside of the bilayer, which is required for spontaneous vesicle formation.[7,13] On the other hand, the dynamic ion exchange facilitates the minimization of the spontaneous curvature required for the L_3 phase formation and, hence, explains its remarkable stability.

The weaker solvophobic effect in EAN as compared to water (e.g., the critical micelle concentration of cetyltrimethylammonium bromide in EAN is ten times larger than in water[18]) combined with the counterion exchange allows the amphiphilic molecules to arrange into closed spherical bilayers, which is the most favorable type of configuration for bilayers (because the energetically and entropically unfavorable edges of planar bilayers are eliminated at a finite, rather than infinite, aggregation number[39]). The high solubility of DDAB in EAN is consistent with the fact that the bilayers contain only a small fraction of the total surfactant, with the rest as monomers in solution. It is well-known that for $1/2 < p < 1$, the smallest vesicle radius that may be formed without forcing the headgroup area of the outer monolayer to exceed a_0 is given by $D_c \approx 2l_c/(1 - p)$.[39] Given that for the large DDAB/EAN vesicles $l_c/R \sim 10^{-3}$, it follows that $p \approx 1$, which implies that the spontaneous curvature is reduced to minimize the free energy.[7,40]

Finally, the Gibbs phase rule applied to this system admits the possibility of 3-phase equilibrium. This might also explain the measured composition difference between the vesicle interior and exterior and may play a role in their formation. Observations, over weeks, however, do not show evidence of formation of a third macrophase. Indeed, vesicle formation is shown to be path independent, and the vesicles formed for all compositions in the two phase region.

■ CONCLUSIONS

In summary, we report the first observations of spontaneous vesicles formation in a protic ionic liquid. The DDAB/EAN vesicles fulfill the three criteria for equilibrium vesicle phases,[7] namely, (1) they are formed spontaneously upon dispersing dry surfactant into EAN without mechanical or chemical perturbation; (2) they do not aggregate with time, and (3)

dx.doi.org/10.1021/ja308975e | J. Am. Chem. Soc. 2012, 134, 20728–20732

they spontaneously reform after reversing any physical or chemical process to which they are exposed (e.g., temperature jumps or changes in concentration). In addition, they form identically independent of the path taken to reach the final vesicle state. Further, spontaneous vesicles are found throughout compositions in the two phase region. Additionally, we observed a coexistence between the L_3 phase and giant vesicles and a dilute phase containing large vesicles, which is confirmed quantitatively by SANS analysis of the phases in equilibrium. The spontaneity of formation and the stability of both the vesicular and L_3 phases are due to a combination of two effects: the weak solvophobic effect of EAN and the dynamic ($Br^--NO_3^-$) ion exchange at the exterior of the bilayer membrane. Because of the very low solubility of DDAB in water, both vesicular and the L_3 phase have only been observed at very small concentrations in the analogous aqueous DDAB solution.[3,4] The ease of preparation of DDAB/EAN vesicles and sponge phase provides many advantages for their potential use as microreactors, microcarries or as templates for the synthesis of mesoporous materials. This research suggests that, given the great variety of possible amphiphile systems, many more can potentially form vesicles. However, a series of systematic studies on the solvophobic effect and the electrostatic interactions in these systems are necessary to fully understand the spontaneous formation of ionic vesicles in ionic liquids.

■ ASSOCIATED CONTENT

Supporting Information

Experimental procedure, complementary BFM analysis, mass balance of DDAB/EAN solutions, structural analysis of GVs and the L_3 phase, rheology of the L_3 phase and movies showing spontaneous and thermoreversible formation of large and giant vesicles. This material is available free of charge via the Internet at http://pubs.acs.org.

■ AUTHOR INFORMATION

Corresponding Author

wagnernj@udel.edu

Present Addresses

[‡]ExxonMobil Chemical Company, Baytown, Texas, 77520, USA

[¶]Department of Chemical Engineering, Indian Institute of Technology, Madras Chennai 600 036, India

Notes

The authors declare no competing financial interest.

■ ACKNOWLEDGMENTS

This manuscript was prepared under cooperative agreement 70NANB7H6178 from the National Institute of Standards and Technology (NIST), US Department of Commerce.

■ REFERENCES

(1) Kunitake, T.; Okahata, Y. *J. Am. Chem. Soc.* **1977**, *99*, 3860−3861.
(2) Olson, F.; Hunt, C. A.; Szoka, F. C.; Vail, W. J.; Papahadjopoulos, D. *Biochim. Biophys. Acta* **1979**, *557*, 9−23.
(3) Dubois, M.; Zemb, T. *Langmuir* **1991**, *7*, 1352−1360.
(4) Caboi, F.; Monduzzi, M. *Langmuir* **1996**, *12*, 3548−3556.
(5) Kaler, E. W.; Murthy, A. K.; Rodriguez, B. E.; Zasadzinski, J. A. *Science* **1989**, *245*, 1371−1374.
(6) Grillo, I.; Penfold, J.; Tucker, I.; Cousin, F. *Langmuir* **2009**, *25*, 3932−3943.
(7) Kaler, E. W.; Herrington, K. L.; Murthy, A. K.; Zasadzinski, J. A. *J. Phys. Chem.* **1992**, *96*, 6698−6707.
(8) Herrington, K. L.; Kaler, E. W.; Miller, D. D.; Zasadzinski, J. A.; Chiruvolu, S. *J. Phys. Chem.* **1993**, *97*, 13792−13802.
(9) Marques, E.; Khan, A.; Miguel, M. D.; Lindman, B. *J. Phys. Chem.* **1993**, *97*, 4729−4736.
(10) Antonietti, M.; Forster, S. *Adv. Mater.* **2003**, *15*, 1323−1333.
(11) Segota, S.; Heimer, S.; Tezak, D. *Colloids Surf., A.* **2006**, *280*, 245−245.
(12) Segota, S.; Tezak, D.; Talmon, Y. *Soft Mater.* **2005**, *3*, 51−69.
(13) Ninham, B. W.; Evans, D. F.; Wei, G. J. *J. Phys. Chem.* **1983**, *87*, 5020−5025.
(14) Brady, J. E.; Evans, D. F.; Kachar, B.; Ninham, B. W. *J. Am. Chem. Soc.* **1984**, *106*, 4280−4282.
(15) Murthy, A. K.; Kaler, E. W.; Zasadzinski, J. A. N. *J. Colloid Interface Sci.* **1991**, *145*, 598−600.
(16) Evans, D. F.; Chen, S.-H.; Schriver, G. W.; Arnett, E. M. *J. Am. Chem. Soc.* **1981**, *103*, 481−482.
(17) Beesley, A. H.; Evans, D. F.; Laughlin, R. G. *J. Phys. Chem.* **1988**, *92*, 791−793.
(18) Evans, D. F.; Yamauchi, A.; Roman, R.; Casassa, E. Z. *J. Colloid Interface Sci.* **1982**, *88*, 89−96.
(19) Bordel-Velasco, S.; Turmine, M.; Caprio, D. D.; Letellier, P. *Colloids Surf., A* **2006**, *275*, 50−54.
(20) Bleasdale, T. A.; Tiddy, G. J. T.; Wyn-Jones, E. *J. Phys. Chem.* **1991**, *95*, 5385−5386.
(21) Araos, M. U.; Warr, G. G. *J. Phys. Chem. B* **2005**, *109*, 14275−14277.
(22) Greaves, T. L.; Weerawardena, A.; Fong, C.; Drummond, C. J. *Langmuir* **2007**, *23*, 402−404.
(23) Nakashima, T.; Kimizuka, N. *Chem. Lett.* **2002**, 1018−1019.
(24) Singh, K.; Marangoni, D. G.; Quinn, J. G.; Singer, R. D. *J. Colloid Interface Sci.* **2009**, *335*, 105−111.
(25) Smirnova, N. A.; Safonova, E. A. *Russ. J. Phys. Chem. A* **2010**, *84*, 1695−1704.
(26) Yuan, J.; Bai, X.; Zhao, M.; Zheng, L. *Langmuir* **2010**, *26*, 11726−11731.
(27) Bai, Z.; Lodge, T. P. *J. Am. Chem. Soc.* **2010**, *132*, 16265−16270.
(28) López-Barrón, C. R.; Basavaraj, M. G.; DeRita, L.; Wagner, N. J. *J. Phys. Chem. B* **2012**, *116*, 813−822.
(29) Zemb, T.; Belloni, L.; Dubois, M.; Marcelja, S. *Prog. Colloid Polym. Sci.* **1992**, *89*, 33−38.
(30) Zemb, T.; Gazeau, D.; Dubois, M.; Gulikkrzywicki, T. *Europhys. Lett.* **1993**, *21*, 759−766.
(31) Schurtenberger, P.; Mazer, N.; Kaenzig, W. *J. Phys. Chem.* **1985**, *89*, 1042−1049.
(32) Egelhaaf, S. U.; Schurtenberger, P. *Phys. Rev. Lett.* **1999**, *82*, 2804−2807.
(33) Leng, J.; Egelhaaf, S. U.; Cates, M. E. *Europhys. Lett.* **2002**, *59*, 311.
(34) Leng, J.; Egelhaaf, S. U.; Cates, M. E. *Biophys. J.* **2003**, *85*, 1624−1646.
(35) Bartlett, P.; Ottewill, R. H. *J. Chem. Phys.* **1992**, *96*, 3306−3318.
(36) Pencer, J.; White, G. F.; Hallett, F. R. *Biophys. J.* **2001**, *81*, 2716−2728.
(37) Teubner, M.; Strey, R. *J. Chem. Phys.* **1987**, *87*, 3195−3200.
(38) Greaves, T. L.; Drummond, C. J. *Chem. Soc. Rev.* **2008**, *37*, 1709−1726.
(39) Israelachvili, J. N. *Intermolecular and Surface Forces*; Academic Press: London; San Diego, CA, 1991.
(40) Helfrich, W. *Z. Naturforsch.* **1973**, *28*, 693−703.